frontiers in Built Environment

ORIGINAL RESEARCH
published: 18 February 2020
doi: 10.3389/fbuil.2020.00012

Pullout Behavior of Different Geosynthetics—Influence of Soil Density and Moisture Content

Fernanda Bessa Ferreira, Castorina Silva Vieira and Maria de Lurdes Lopes*

Construct-GEO, Faculty of Engineering, University of Porto, Porto, Portugal

Geosynthetics have increasingly been used as reinforcement in permanent earth structures, such as road and railway embankments, steep slopes, retaining walls, and bridge abutments. The understanding of soil-geosynthetic interaction is of primary importance for the safe design of geosynthetic-reinforced soil structures, such as those included in transportation infrastructure projects. In this study, the pullout behavior of three different geosynthetics (geogrid, geocomposite reinforcement, and geotextile) embedded in a locally available granite residual soil is assessed through a series of large-scale pullout tests involving different soil moisture and density conditions. Test results show that soil density is a key factor affecting the reinforcement pullout resistance and the failure mode at the interface, regardless of geosynthetic type or soil moisture content. The soil moisture condition may considerably influence the pullout response of the geosynthetics, particularly when the soil is in medium dense state. The geogrid exhibited higher peak pullout resistance than the remaining geosynthetics, which is associated with the significant contribution of the passive resistance mobilized against the geogrid transverse members to the overall pullout capacity of the reinforcement.

Keywords: geosynthetics, geosynthetic-reinforced soil structures, pullout behavior, soil moisture content, soil density

OPEN ACCESS

Edited by:
Sanjay Shrawan Nimbalkar, University of Technology Sydney, Australia

Reviewed by:
Amarnath M. Hegde, Indian Institute of Technology Patna, India
Ting Li, Southwest Jiaotong University, China

****Correspondence:***
Castorina Silva Vieira
cvieira@fe.up.pt

Specialty section:
This article was submitted to Transportation and Transit Systems, a section of the journal Frontiers in Built Environment

Received: *06 December 2019*
Accepted: *30 January 2020*
Published: *18 February 2020*

Citation:
Ferreira FB, Vieira CS and Lopes ML (2020) Pullout Behavior of Different Geosynthetics—Influence of Soil Density and Moisture Content. Front. Built Environ. 6:12. doi: 10.3389/fbuil.2020.00012

INTRODUCTION

Geosynthetics have been widely used as a reinforcement material in several geotechnical engineering applications, such as roadway and railway layers and embankments (Wu et al., 1992; Ashmawy and Bourdeau, 1995; Lee and Wu, 2004; Ravi et al., 2014; Ferreira et al., 2016a; Nimbalkar and Indraratna, 2016; Indraratna et al., 2018, 2019; Ngo et al., 2018; Byun and Tutumluer, 2019; Tatsuoka, 2019). In such applications, the interaction mechanism between the geosynthetic and the surrounding material is of primary importance. Recognizing the proper interaction mechanism (shear or pullout) and the selection of the most appropriate test for its characterization are key factors in the design of the above-mentioned structures. When the geosynthetic tends to be pulled out from the reinforced mass (e.g., in the upper zone of a reinforced soil slope or in geosynthetic basal reinforcement), the interaction mechanism shall be characterized through laboratory or field pullout tests.

By definition, the pullout resistance of a geosynthetic is the tensile load required to cause outward sliding of the geosynthetic through the reinforced soil mass. The pullout mechanism of a geogrid differs from that of a geotextile (with continuous surface). In the case of the geogrid,

the pullout resistance is composed of skin friction on the surface of the geogrid ribs (frictional resistance) and bearing resistance mobilized against the transverse members (passive resistance). For geotextiles (with continuous surface), only the frictional resistance contributes to the overall pullout capacity.

The great relevance of the interaction mechanism between the geosynthetic and the surrounding soil is patent in the high number of studies that have been published in the last decades. Several experimental studies related to the fundamentals of soil–geosynthetic interaction under pullout loading conditions have been reported (Raju, 1995; Lopes and Ladeira, 1996a; Palmeira, 2004; Moraci and Recalcati, 2006; Subaida et al., 2008; Tang et al., 2008; Hatami and Esmaili, 2015; Ferreira et al., 2016b, 2020; Mirzaalimohammadi et al., 2019; Morsy et al., 2019; Isik and Gurbuz, 2020). However, despite the wide range of studies available in the literature, most of them have been carried out using freely draining granular soils. The pullout behavior of geosynthetics when inserted in cohesive or residual soils has not been widely explored (Bakeer et al., 1998; Abu-Farsakh et al., 2006; Esmaili et al., 2014; Ferreira et al., 2016b) and more insights are needed.

This paper extends previous work on the pullout response of geosynthetics embedded in granite residual soil presented in Ferreira et al. (2016b). While the earlier study was carried out using dry soil, this current study involves soil compacted at the optimum moisture content, which more closely represents typical field conditions. Special emphasis is placed on the effects of soil dry density, moisture content and geosynthetic type on the pullout resistance and deformation behavior of the reinforcement when subjected to pullout loading. The obtained results will be useful to establish appropriate design parameters for geosynthetic-reinforced soil structures, such as those included in transportation infrastructure projects.

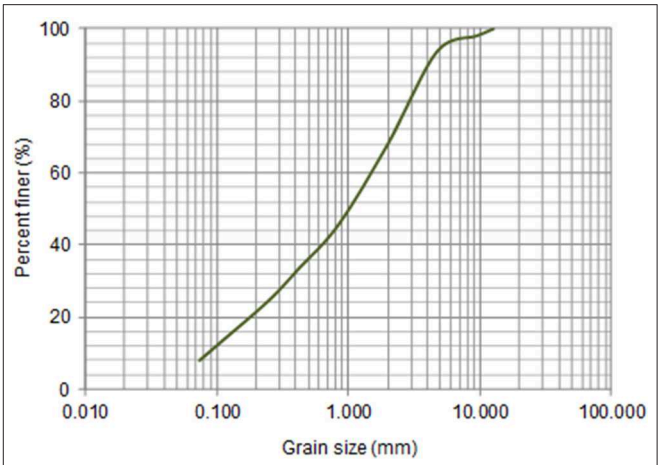

FIGURE 1 | Particle size distribution curve of the granite residual soil.

TABLE 1 | Physical properties of the granite residual soil.

Property	Unit	Value
D_{10}	mm	0.09
D_{30}	mm	0.35
D_{50}	mm	1.00
C_U	–	16.90
C_C	–	1.00
G	–	2.73
e_{max}[a]	–	0.998
e_{min}[a]	–	0.476
γ_{dmax}[b]	kN/m^3	18.93
w_{opt}[b]	%	11.45

[a] *Evaluated using the ASTM D 4253-93 (1993) and ASTM D 4254-93 (1993) standards.*
[b] *Evaluated using the Modified Proctor test [BS 1377-4:1990 (BSI, 1990)].*

MATERIALS AND METHODS

Materials

Soil

Granite residual soils are widely available in the northern region of Portugal and often used as backfill material for reinforced soil construction and sub-base layers of transportation infrastructures. In this regard, a locally available granite residual soil was procured from a local supplier and used throughout the current study. This soil can be classified as SW-SM (well-graded sand with silt and gravel) as per the Unified Soil Classification System (ASTM D 2487-11, 2011). The particle size distribution of this particular soil is presented in **Figure 1** and the main physical properties are summarized in **Table 1**.

Geosynthetics

Three different geosynthetics were analyzed in the present study (**Figure 2**): a biaxial woven geogrid (GGR), a uniaxial high-strength geotextile, commonly referred to as geocomposite reinforcement (GCR) and a non-woven geotextile (GTX). The GGR (**Figure 2A**) is manufactured from high-tenacity polyester yarns, which are covered with a protective polymeric coating. The GCR (**Figure 2B**) is composed of high-tenacity polyester yarns attached to a continuous filament non-woven polypropylene geotextile. The GTX (**Figure 2C**) consists of mechanically bonded (needle punched) continuous filaments of polypropylene.

Several laboratory and field studies have shown the beneficial effect of using non-woven geotextiles as reinforcement elements of fine-grained soils (poorly draining soils) due to their internal drainage capacity (Tan et al., 2001; Portelinha et al., 2013). Indeed, the hydraulic properties of non-woven geotextile reinforcements can assist in the pore-water pressure dissipation, hence improving the internal stability of the reinforced structure. Therefore, a non-woven geotextile and a geocomposite reinforcement (consisting of a non-woven geotextile reinforced with polyester yarns) were selected for the current study.

The in-isolation tensile strength of the geosynthetics was assessed through wide-width tensile tests, following the EN ISO 10319:2008 (CEN, 2008). The mean load-strain curves from five tensile tests carried out under repeatability conditions for each geosynthetic are shown in **Figure 3**. A summary of the relevant physical and mechanical properties of the reinforcements is given in **Table 2**.

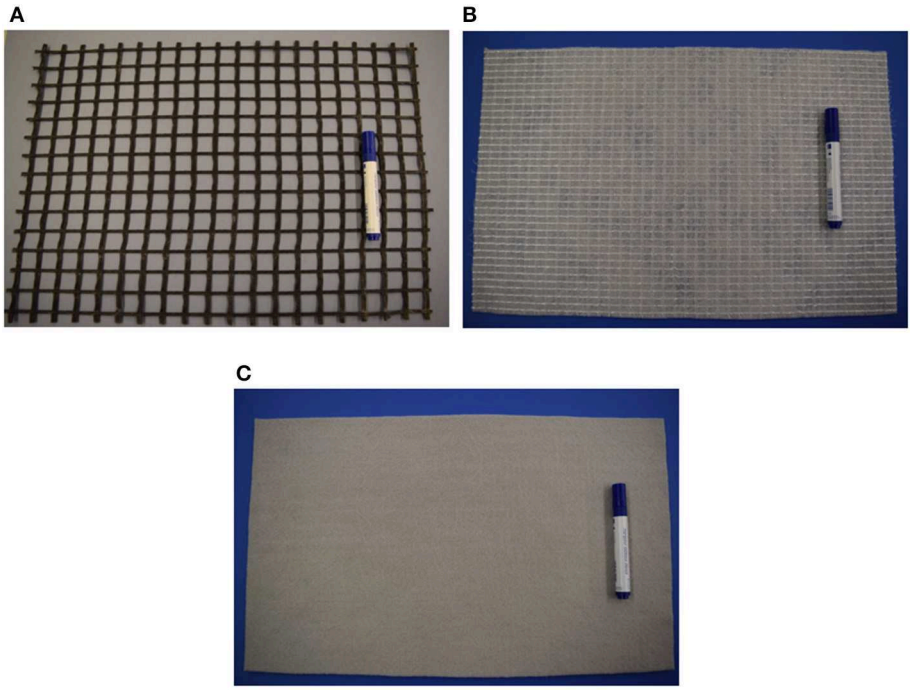

FIGURE 2 | Geosynthetics used: **(A)** GGR; **(B)** GCR; **(C)** GTX.

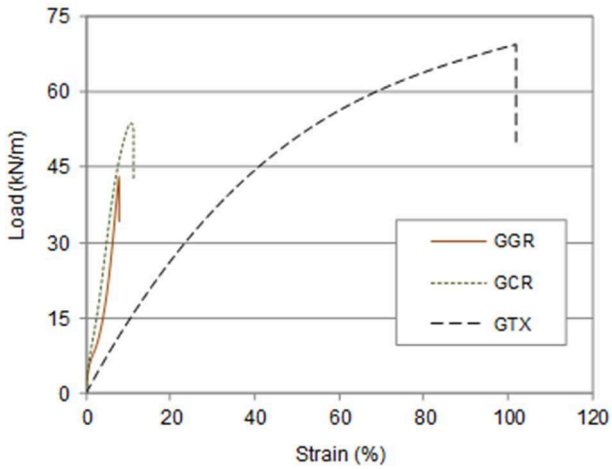

FIGURE 3 | Mean load-strain curves of the geosynthetics from in-isolation tensile tests performed according to EN ISO 10319:2008 (CEN, 2008).

TABLE 2 | Physical and mechanical properties of the geosynthetics.

Property	Unit	Geosynthetics		
		GGR	GCR	GTX
Raw material	–	PET	PET/PP	PP
Mass per unit area	g/m^2	380	310	1,000
Thickness-2 kPa	mm	–	2.3	7.2
Thickness of longitudinal ribs	mm	1.6	–	–
Thickness of transverse ribs	mm	1.6	–	–
Mean grid size	mm	25 × 25	–	–
Percent open area	%	68	–	–
Short term tensile strength[a]	kN/m	58	58	55
Elongation at maximum load[a]	%	10.5	11.5	105.0
Short term tensile strength[b]	kN/m	43.9	54.6	69.5
Elongation at maximum load[b]	%	7.9	10.6	100.9
Secant stiffness at 5% strain[b]	kN/m	401.6	600.9	156.3

[a] *As per the manufacturer specifications (machine direction).*
[b] *Obtained from tensile tests performed in accordance with EN ISO 10319:2008 (CEN, 2008).*

Pullout Test Device and Experimental Procedures

The large-scale pullout test apparatus used in the present study is illustrated in **Figure 4A**. The equipment consists of a large pullout box (internal dimensions of 1.53 m long × 1.00 m wide × 0.80 m high) fitted with a 0.20 m long (steel) sleeve, a clamping system (**Figure 4B**), a servo-hydraulic control system and a set of external transducers, such as load cells and potentiometers. A detailed description of the test facility can be found elsewhere (Lopes and Ladeira, 1996b; Ferreira et al., 2016b).

The pullout tests herein reported were performed in accordance with the European Standard EN 13738:2004 (CEN, 2004). For tests involving moist soil, the soil was thoroughly mixed with water to achieve the target moisture content and ensure the homogeneity of the sample. The soil was then compacted inside the pullout box to the required density in

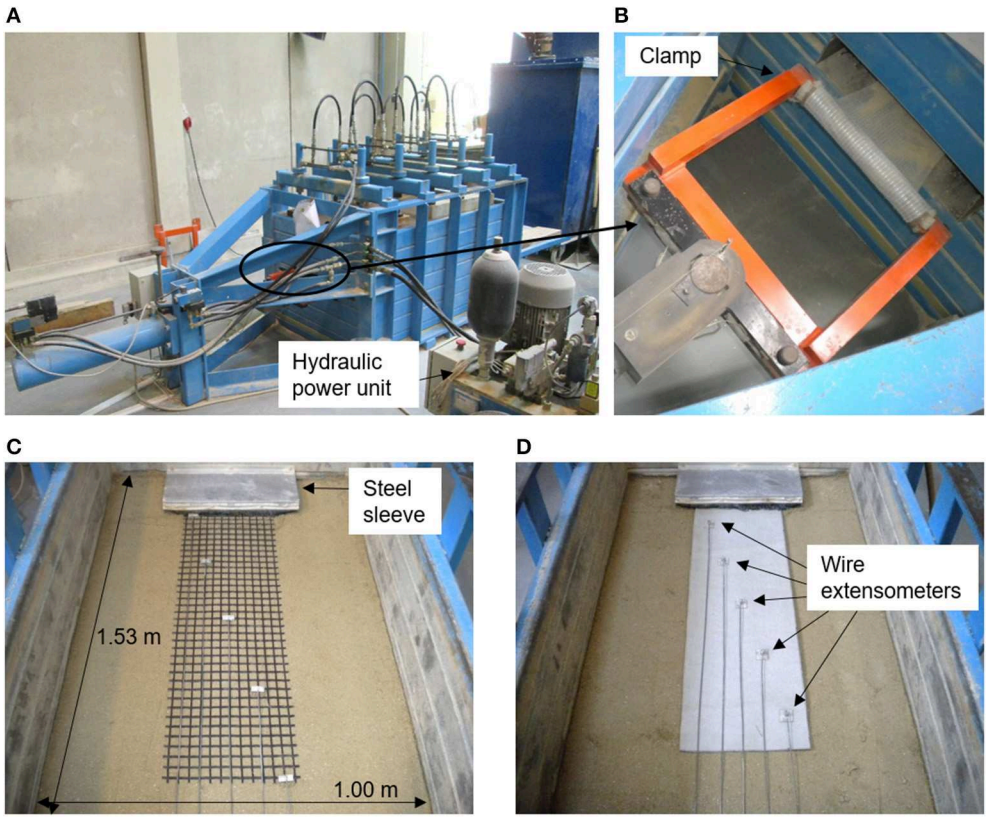

FIGURE 4 | Large-scale pullout test apparatus and instrumentation: **(A)** overall view; **(B)** clamping system; **(C)** inextensible wires fixed along a GGR specimen; **(D)** inextensible wires fixed along a GTX specimen.

0.15 m thick layers using an electric vibratory hammer. Once the first two layers were compacted, the geosynthetic specimen (with initial dimensions of 0.33 m wide and 1.0 m long) was clamped and laid over the compacted soil. To monitor the horizontal displacements along the length of the reinforcement during the test, a set of wire extensometers were fixed to the geosynthetic at selected measurement points (**Figures 4C,D**), with the opposite ends connected to linear potentiometers located at the back of the pullout box. Two additional soil layers were then placed and compacted, which resulted in a total height of soil of 0.60 m. A neoprene sheet was installed between the soil and the loading plate to reduce the influence of the top boundary and obtain more uniform distribution of the vertical stresses. The vertical load was applied to the upper layer of soil by a wooden plate loaded by 10 hydraulic jacks and its magnitude was controlled by a load cell. The pullout force was then applied to the geosynthetic specimen so as to achieve a constant rate of displacement of 2 mm/min, as recommended by the EN 13738:2004 (CEN, 2004). It should be noted that the recommended displacement rate for geosynthetic pullout testing varies according to different standards. For instance, the American Standard ASTM D6706-01 (2013) suggests the use of a displacement rate of 1 mm/min. Even though the rate of displacement under which the pullout tests are carried out may influence the results, the evaluation of this effect was beyond the scope of this study. The geosynthetic frontal displacement (i.e., clamp displacement) and the associated pullout force were measured by a linear potentiometer and a load cell, respectively. An automatic data acquisition system enabled the relevant parameters (i.e., the pullout force, frontal displacement, displacements throughout the length of the geosynthetic specimen, and the applied vertical stress) to be continuously monitored during the tests. To ensure accuracy of results, all the measurement devices have undergone calibration prior to testing.

Test Programme

Table 3 summarizes the test conditions investigated in this study. As previously mentioned, the pullout response of three distinct geosynthetics (geogrid, geocomposite reinforcement, and geotextile) when embedded in a locally available granite residual soil was assessed using a large pullout box. To analyse the influence of soil moisture content on the pullout resistance and deformation behavior of the reinforcements, the soil was tested in its air-dried moisture condition and at the optimum moisture content ($w_{opt} = 11.45\%$). In addition, two different dry densities were investigated: $\gamma_d = 15.3$ kN/m^3 (medium dense soil) and $\gamma_d = 17.3$ kN/m^3 (dense soil). To simulate low depths, where the pullout failure mechanism is most likely to occur in reinforced soil walls and slopes, all the tests were performed under a relatively low vertical stress at the reinforcement level

TABLE 3 | Test programme.

Test	Geosynthetic	Soil moisture content	Soil dry unit weight (kN/m^3)	Vertical stress (kPa)	Number of specimens
T1	GGR	Dry	15.3	25	3
T2	GGR	Dry	17.3	25	3
T3	GGR	w_{opt}	15.3	25	3
T4	GGR	w_{opt}	17.3	25	3
T5	GCR	Dry	15.3	25	3
T6	GCR	Dry	17.3	25	3
T7	GCR	w_{opt}	15.3	25	3
T8	GCR	w_{opt}	17.3	25	3
T9	GTX	Dry	15.3	25	3
T10	GTX	Dry	17.3	25	3
T11	GTX	w_{opt}	15.3	25	3
T12	GTX	w_{opt}	17.3	25	3

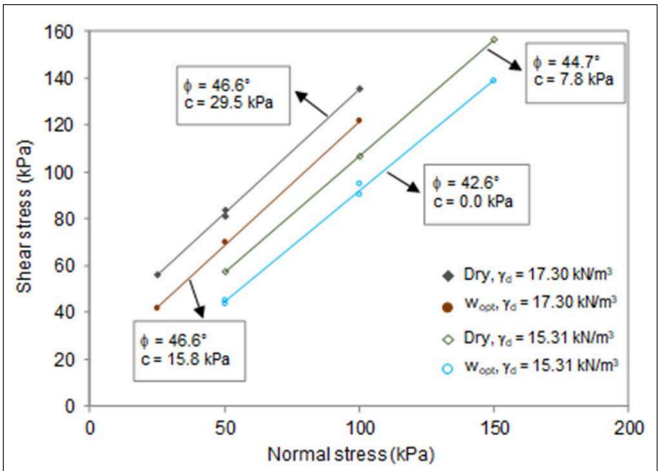

FIGURE 5 | Peak strength envelopes of the granite residual soil [modified from Ferreira et al. (2015)].

(σ_v = 25 kPa). As recommended by the EN 13738:2004 (CEN, 2004), each test was carried out three times under identical physical conditions, to ensure repeatability of results. Therefore, 36 geosynthetic specimens were tested.

Additionally, large-scale direct shear tests were carried out to evaluate the internal shear strength of the soil. The direct shear tests were also performed for different conditions of moisture content (air-dried and optimum moisture content) and dry density (γ_d = 15.3 kN/m^3 and γ_d = 17.3 kN/m^3) and under normal stresses ranging from 25 to 150 kPa. The direct shear test apparatus used in this study enables the analysis of the direct shear behavior of soils, as well as soil-geosynthetic and geosynthetic-geosynthetic interfaces. The direct shear box comprises a lower box with dimensions of 800 × 340 mm in plan and 100 mm in height, and an upper box with plan dimensions of 600 × 300 mm and 150 mm in height. Details on this large-scale direct shear prototype can be found elsewhere (Vieira et al., 2013; Ferreira et al., 2015).

RESULTS AND DISCUSSION

Soil Internal Shear Strength

Figure 5 plots the maximum shear stresses mobilized in the direct shear tests as function of the normal stress, along with the corresponding linear best-fit lines, for different conditions of soil moisture content and dry density. Due to limitations of the fluid power unit, the direct shear tests for dense soil (γ_d = 17.3 kN/m^3) were carried out for the range 25−100 kPa.

Following the Mohr-Coulomb failure criterion, the peak shear strength parameters of the soil (i.e., internal friction angle, ϕ and cohesion, c) were obtained. As expected, the soil shear strength increased significantly with the placement density, with more emphasis on the cohesive component of the shear strength. On the other hand, the increase in soil moisture content adversely affected the soil internal strength. In fact, although the soil friction angle was not significantly affected by the moisture condition, the cohesion decreased considerably when the soil was tested at its optimum moisture content. According to Mitchell (1976) and Samtani and Nowatzki (2006), apparent cohesion in soils may derive from two main factors: (1) capillary stresses between particles in an unsaturated soil due to surface tension in the water (matric suction) and (2) apparent mechanical forces resulting from interlocking of angular soil particles, which is often the cause of cohesion measured in compacted soils (i.e., particle geometry and packing may induce an apparent cohesion with no physical or chemical attraction between soil particles). Therefore, the increment of cohesion observed in this study when the dry density of the soil changed from 15.3 to 17.3 kN/m^3 may be associated with an increase of the apparent mechanical forces due to enhanced interlocking of soil particles. On the other hand, the decrease of cohesion associated with an increase in soil moisture content is possibly related to the loss of soil matric suction.

Pullout Test Results

Influence of Soil Moisture Content

Figure 6 illustrates the effect of soil moisture content on the pullout resistance of the geosynthetics for different soil dry unit weights (γ_d = 15.3 kN/m^3 and γ_d = 17.3 kN/m^3). **Figures 6A,B** show the pullout force-displacement curves obtained when the geogrid reinforcement was tested in looser and denser soil specimens, respectively. Similarly, **Figures 6C,D** present the results obtained for the geocomposite reinforcement and **Figures 6E,F** plot the data concerning the geotextile.

Figures 6A,B indicate that the pullout resistance of the geogrid embedded in dry soil exceeded that for soil compacted at the optimum moisture content (at the same dry density). It can also be observed that the influence of soil moisture content on the geogrid pullout response was more pronounced when the soil was in medium dense conditions (**Figure 6A**). In fact, for γ_d = 15.3 kN/m^3 (**Figure 6A**), the peak pullout resistance (P_R) of the reinforcement decreased about 19% (on average) with the moisture content increase. However, for dense soil

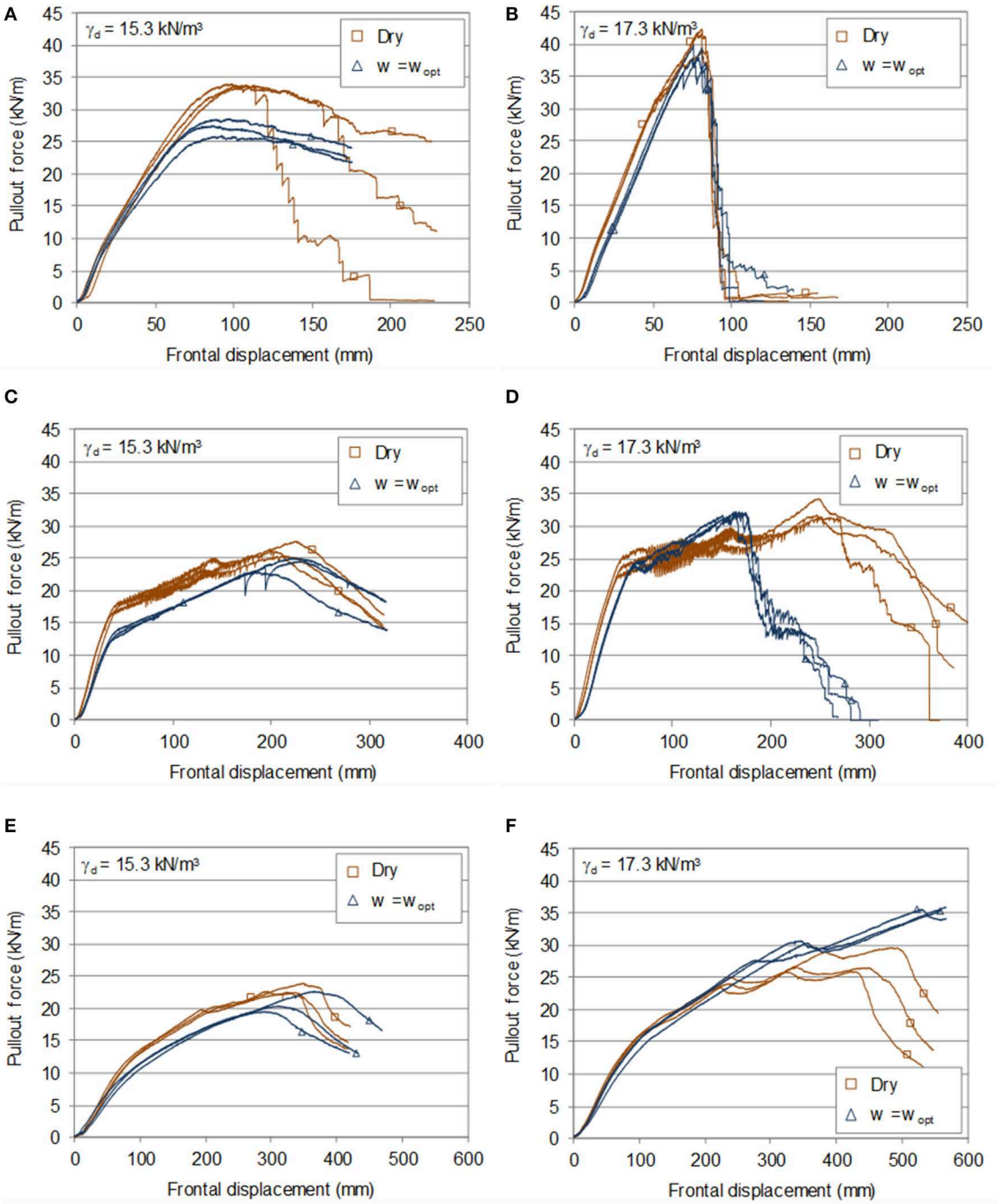

FIGURE 6 | Influence of soil moisture content on the pullout resistance of the geosynthetics: **(A,B)**: GGR; **(C,D)**: GCR; **(E,F)**: GTX.

(γ_d = 17.3 kN/m^3), the reduction of P_R due to the moisture content increase was only 7% (**Figure 6B**). This finding may be attributed to the different failure modes observed in these tests. In the tests involving medium dense soil, the failure occurred due to sliding of the reinforcement along the interface (pullout failure). In contrast, for dense soil, the specimens failed in tension (tensile failure).

Figure 6C shows that the increase in soil moisture content led to the reduction (8.5%) of the pullout resistance of the geocomposite reinforcement when embedded in medium dense soil. This reduction was considerably lower than that observed for the geogrid under identical conditions, which may be related to the favorable hydraulic properties of non-woven geotextiles (Ling et al., 1992; Tan et al., 2001; Portelinha et al., 2013). However, for

dense soil (**Figure 6D**) the moisture content did not significantly affect the peak pullout capacity of the geosynthetic (over the investigated range), but the frontal displacement at which the peak pullout resistance was mobilized decreased substantially when the optimum moisture content was tested.

The influence of soil moisture condition on the pullout response of the geotextile in medium dense soil was similar to that observed for the geocomposite. When the soil was compacted at the optimum moisture content, the peak pullout resistance decreased 9.4% (on average) in comparison with that obtained in the presence of dry soil (**Figure 6E**). As shown in **Figure 6F**, for dense soil it was not possible to evaluate the peak pullout resistance of the geotextile for $w = w_{opt}$, since a higher frontal displacement would be required to reach the ultimate capacity. Nevertheless, it can be concluded that the pullout resistance of this geotextile under these particular test conditions increased with moisture content (from air-dried to optimum moisture content), which contrasts with the behavior observed for the remaining geosynthetics. This is possibly associated with the high thickness of the geotextile (thickness = 7.2 mm) and the significant intrusion of soil particles into the geotextile pores during compaction at $w = w_{opt}$, thus leading to its higher tensile stiffness under moist conditions.

Influence of Soil Density

The effect of soil placement density on the pullout resistance of the different geosynthetics and on the average displacements recorded along the specimens at maximum pullout force is shown in **Figure 7**. **Figures 7A,B** present the results attained for the geogrid, while **Figures 7C,D** correspond to the geocomposite reinforcement. The results for the geotextile are shown in **Figures 7E,F**. Although the data in **Figure 7** were obtained for $w = w_{opt}$, similar conclusions were also drawn regarding the influence of soil density on the pullout load-displacement behavior of the geosynthetics when the soil was tested in its air-dried moisture condition.

Figures 7A,B clearly show that soil density is a key factor affecting the pullout behavior of the geogrid. The increase in soil density resulted in an increment of the pullout resistance of the geogrid of about 40% (**Figure 7A**). The secant stiffness at a pullout force corresponding to 50% of the maximum pullout resistance increased 14% with soil density. In turn, the frontal displacement at which the ultimate pullout load was achieved decreased about 16%. Soil density also affected the failure mode observed in the tests. For specimens tested in medium dense soil, the failure resulted from sliding of the reinforcement along the interface (i.e., pullout failure, see **Figure 8A**). In contrast, the specimens embedded in dense soil experienced tensile failure (i.e., breakage of the material in tension, see **Figure 8B**).

The profiles of the displacements measured throughout the length of the geogrid at maximum pullout force (plotted in **Figure 7B**) indicate that, for medium dense soil the reinforcement experienced pullout movement during the test (reflected by the displacement measured at the rear end of the specimens). However, for dense soil the displacements recorded over the geogrid length were mainly caused by the reinforcement deformation at the front half of its length (i.e., close to the point of application of the pullout load). In fact, neither sliding nor appreciable deformation at the back half of the geogrid length were observed in the tests involving dense soil. It can therefore be concluded that soil density restrained the transfer of stresses throughout the length of the geogrid specimens and high stresses/strains were mobilized close to the loaded end, thus leading to tensile failure of the specimens at the front part.

The influence of soil placement density on the pullout resistance of the geocomposite reinforcement (**Figure 7C**) was comparable to that for the geogrid. The maximum pullout force increased ∼33% with soil density, whereas the frontal displacement at peak decreased 22%. The secant stiffness for 50% of the maximum pullout force increased about 26% with soil density. The displacement distributions along the length of the specimens at maximum load (**Figure 7D**) indicate that, regardless of density, the deformations tended to decrease with increasing distance to the point of application of the pullout load. At the back of the geocomposite specimens, higher deformations were obtained for specimens tested in looser soil. This is associated with the effect of soil density, which restrains the transfer of stresses over the length of the specimens. Similar to the trend observed for the geogrid, soil density also affected the failure mode observed in these tests. The geocomposite specimens experienced pullout failure when embedded in medium dense soil, whereas for dense soil the specimens underwent internal rupture in tension.

It can be noted from **Figure 7E** that the pullout capacity of the geotextile embedded in dense soil could not be determined, since the maximum admissible frontal displacement was not enough to reach the peak load. Considering the maximum pullout force measured at the end of the test as the lower limit of the pullout resistance of this geotextile, it becomes apparent that the pullout resistance increased at least 70% with soil density. The deformations along the first three sections of the geotextile embedded in dense soil exceeded those for the specimens tested in looser soil. However, identical deformations were measured along the two sections closer to the back end of the specimens, regardless of soil density (**Figure 7F**).

Influence of Geosynthetic Type

Figures 9, **10** compare the pullout behavior of the three geosynthetics in looser and denser soil specimens. **Figure 9** presents the results for dry soil and **Figure 10** is related to soil optimum moisture content. The graphs on the left side show the pullout force-displacement curves and the graphs on the right side illustrate the displacements over the length of the geosynthetics at maximum pullout load.

Regardless of the conditions of soil moisture content and density, the geogrid exhibited significantly higher performance than the other geosynthetics in terms of peak pullout resistance and stiffness. This is associated with the relevant contribution of the passive resistance mechanism mobilized against the geogrid transverse members to the overall pullout capacity of the reinforcement. However, for small displacements, the geogrid stiffness was rather similar to that of the geocomposite reinforcement, suggesting that the latter geosynthetic may be as effective as the geogrid in applications where high deformation

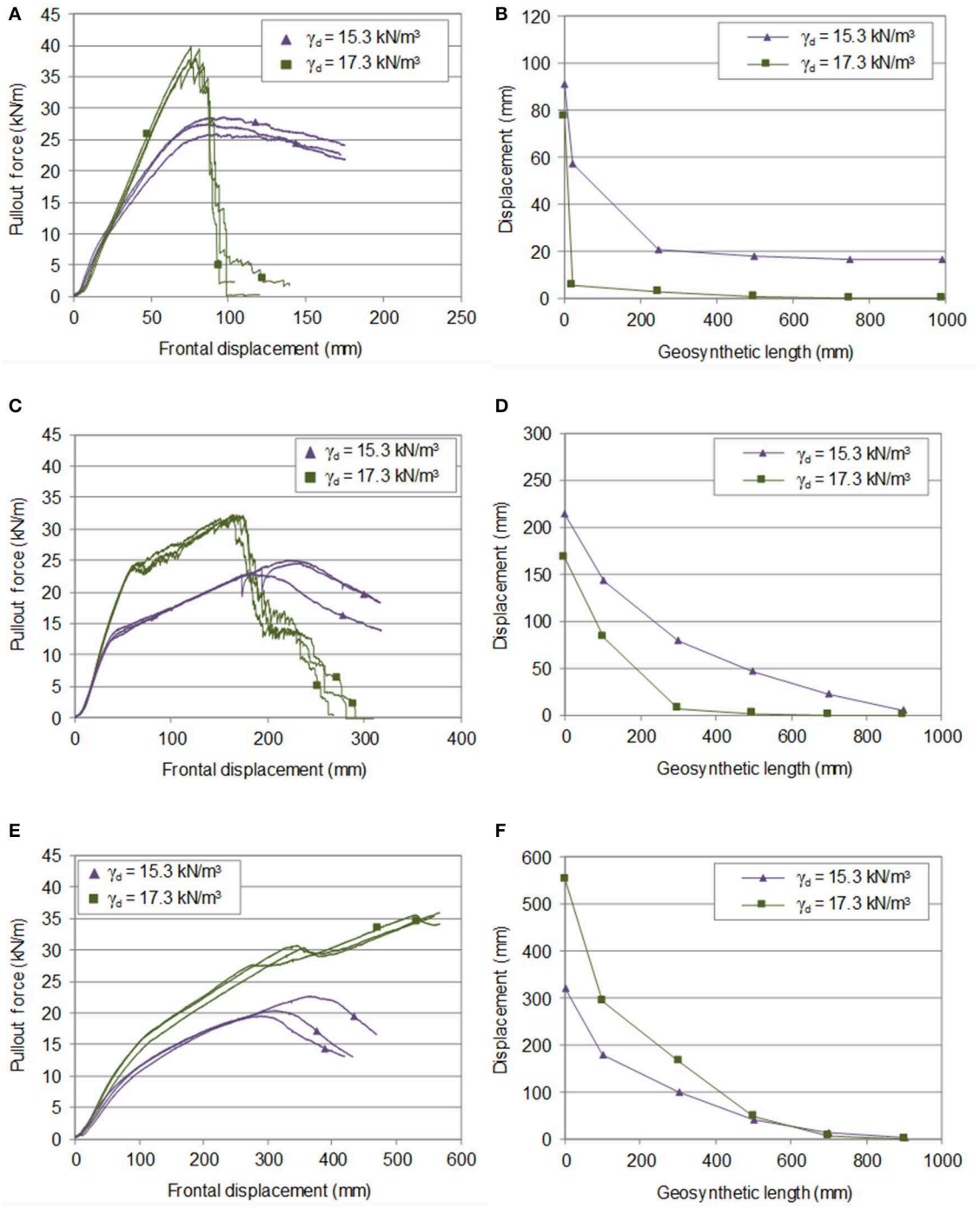

FIGURE 7 | Influence of soil density on the pullout resistance and displacement behavior of the geosynthetics for $w = w_{opt}$: **(A,B)**: GGR; **(C,D)**: GCR; **(E,F)**: GTX.

levels are not anticipated. On the other hand, the stiffness of the geotextile was clearly lower than that of the geogrid and the geocomposite, and hence the frontal displacement at which the maximum pullout force was achieved was substantially larger when the geotextile was used. This is associated with the higher extensibility of this geosynthetic, as previously observed from the in-isolation tensile tests (significantly lower tensile stiffness—**Table 2**).

Comparing the displacements measured throughout the length of the reinforcements at maximum load, it can be concluded that the deformations along the geotextile and the geocomposite reinforcement were significantly larger than those along the geogrid, regardless of the test conditions. This occurrence can be attributed to the higher extensibility of the geotextiles and the fact that the ultimate pullout load is reached at significantly larger frontal displacements.

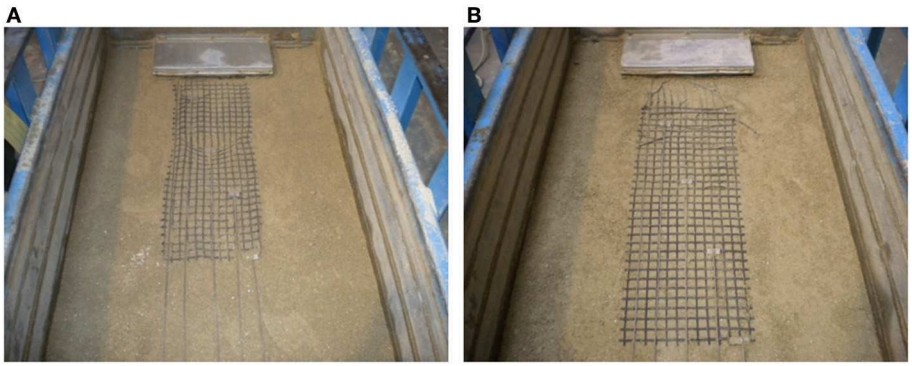

FIGURE 8 | Photographic views of two representative geogrid specimens: **(A)** after pullout failure; **(B)** after tensile failure.

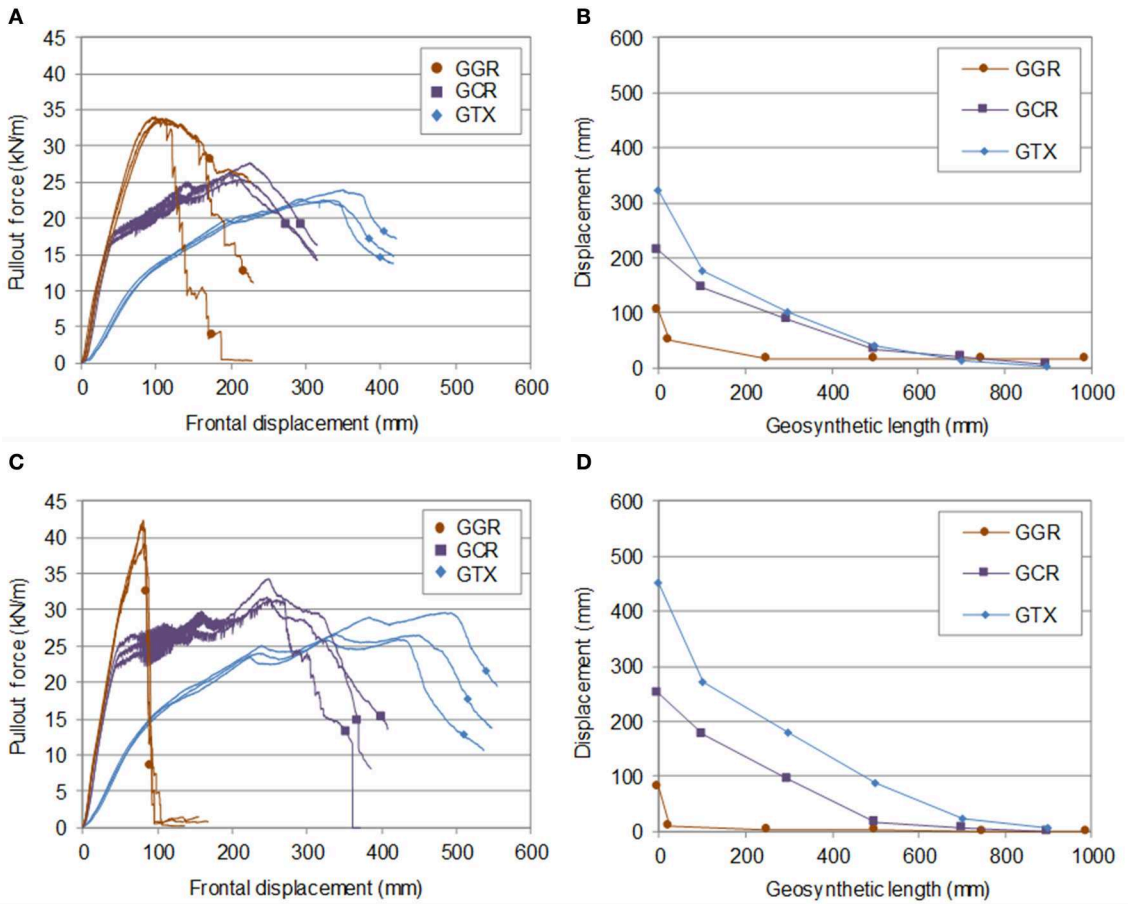

FIGURE 9 | Influence of geosynthetic type on the pullout resistance and displacement behavior of the specimens for dry soil: **(A,B)**: γ_d = 15.3 kN/m^3; **(C,D)**: γ_d = 17.3 kN/m^3.

DISCUSSION

Table 4 summarizes the results of the pullout test programme. The mean values of the pullout resistance (P_R), the frontal displacement for P_R (u_{PR}), and the in-soil secant stiffness for 50% of P_R (J_{50}) are reported in this table, along with the corresponding coefficients of variation (COV), which were computed as the ratio of the standard deviation to the mean value of the parameter, based on three repeatability tests. The conditions of each test can be found in **Table 3**.

Regardless of the geosynthetic or soil moisture content, the increase in soil density led to an increase in the pullout

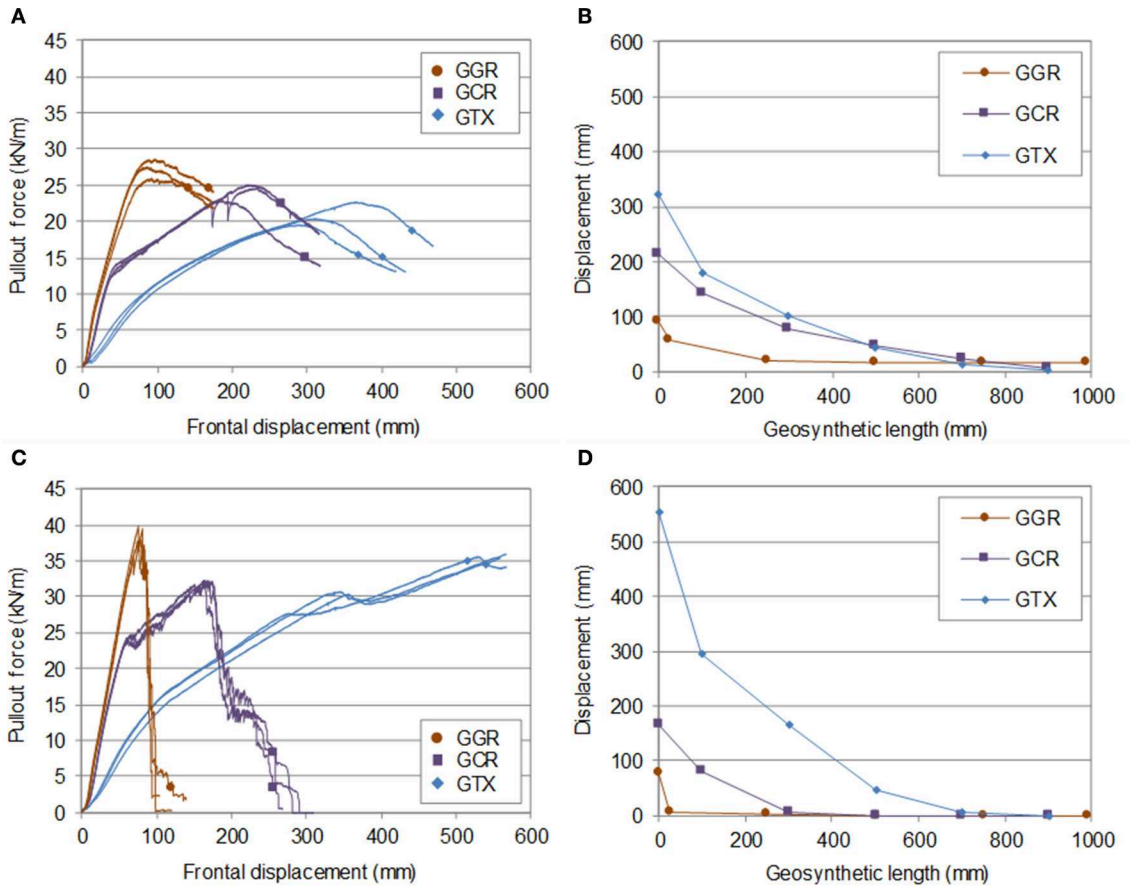

FIGURE 10 | Influence of geosynthetic type on the pullout resistance and displacement behavior of the specimens for $w = w_{opt}$: **(A,B)**: $\gamma_d = 15.3$ kN/m^3; **(C,D)**: $\gamma_d = 17.3$ kN/m^3.

TABLE 4 | Summary of pullout test results.

Test	Pullout resistance (P_R)		Frontal displacement (u_{PR})		Secant stiffness (J_{50})	
	Mean value (kN/m)	COV (%)	Mean value (mm)	COV (%)	Mean value (kN/m)	COV (%)
T1	33.78	0.95	104.55	7.02	461.95	6.50
T2	41.09	4.23	80.47	2.17	613.27	2.51
T3	27.40	4.82	91.47	5.86	444.35	5.38
T4	38.37	3.53	77.20	2.18	506.13	3.92
T5	26.44	4.30	212.04	6.08	458.60	7.08
T6	32.51	4.82	251.37	2.78	562.50	5.61
T7	24.20	4.85	213.82	11.23	336.24	4.30
T8	32.15	0.67	166.58	2.18	424.54	2.03
T9	23.08	3.32	321.80	8.56	143.88	5.22
T10	27.39	7.22	449.86	7.17	168.67	1.96
T11	20.91	7.77	322.53	11.94	116.06	9.36
T12	>35.65	0.76	>551.83	3.48	131.54	8.01

resistance, P_R and secant stiffness, J_{50}. The geogrid (GGR) and the geocomposite (GCR) failed in tension (tensile failure) in denser soil at $w = w_{opt}$ (see **Figure 7** and **Table 5**), which justifies the lower frontal displacements for P_R. In general, the soil moisture content increase (from dry to optimum) induced a decrease in the pullout resistance, P_R and secant stiffness, J_{50}.

When the soil is reinforced with geosynthetics, the interface strength is typically characterized through coefficients of

interaction. The pullout interaction coefficient (f_b) can be defined as:

$$f_b = \frac{\tau^{max}_{pullout}(\sigma)}{\tau^{max}_{direct\ shear}(\sigma)} \quad (1)$$

where $\tau^{max}_{pullout}(\sigma)$ is the maximum shear stress mobilized at the soil-geosynthetic interface during a pullout test under the confining pressure σ, and $\tau^{max}_{direct\ shear}(\sigma)$ is the soil direct shear strength under the same confining pressure.

The mean values of $\tau^{max}_{pullout}(\sigma)$, $\tau^{max}_{direct\ shear}(\sigma)$ and f_b obtained for each test condition are listed in **Table 5**. Also included in this table is the failure mode for each specimen (values in brackets represent the number of specimens). As shown in **Table 5**, the soil-geosynthetic pullout interaction coefficients ranged from 0.25 to 0.61. Under similar conditions, the geogrid exhibited higher pullout interaction coefficients, followed by the geocomposite reinforcement (test T1–T4 and T5–T8, respectively). It is noteworthy that for dense soil (tests T2, T4, and T8), the failure of the geogrid and the geocomposite occurred due to their internal breakage, and thus the coefficients of interaction provided in **Table 5** represent a lower bound for f_b.

A wide range of pullout interaction coefficients can be found in the literature. However, it is important to bear in mind that the pullout interaction coefficient depends on the shear strength of the surrounding soil, the friction between the soil and the geosynthetic, the percent open area, the ratio between the soil grain size and the geogrid aperture, the strength of the junctions, among other factors. For instance, Hsieh et al. (2011) reported values of the pullout interaction coefficient ranging from 0.18 to 1.25 from pullout tests of geosynthetics inserted in different granular soils. Pullout interaction coefficients varying from 0.44 to 1.04 were reported by Mohiuddin (2003) for different geosynthetics embedded in a cohesive soil. Vieira et al. (2016) presented values ranging from 0.58 to 0.63 for geogrids embedded in a recycled construction and demolition material.

Comparing the values of the pullout interaction coefficient achieved in the present study with those reported in the literature, it is possible to conclude that the upper bound of the range is generally lower. This may be due to the occurrence of geosynthetic tensile failure (breakage of the material in tension) when the specimens were embedded in dense soil.

Tables 4, **5** indicate that when the geosynthetics underwent tensile failure under pullout loading conditions, the measured peak pullout force was lower than the corresponding tensile strength obtained through in-isolation tensile tests (**Table 2**). This finding is in agreement with some previous related studies (Lopes and Ladeira, 1996a; Ferreira et al., 2016b; Vieira et al., 2016). It should be noted that in the pullout test the geosynthetic specimen is in contact with compacted soil and under a prescribed normal stress. In contrast, in the tensile test the specimen is tested under unconfined conditions. Furthermore, in the current study, the tensile and pullout tests were performed under different displacement rates. The displacement rates imposed in the tensile (20%/min) and pullout tests (2 mm/min) followed the recommendations of the European Standards EN ISO 10319:2008 (CEN, 2008) and EN 13738:2004 (CEN, 2004), respectively. Therefore, the comparatively lower forces reached in the pullout tests where reinforcement tensile failure occurred may be associated with the different test conditions, as well as some damage induced by the soil on the geosynthetic specimens.

TABLE 5 | Determination of the pullout interaction coefficient (f_b) and failure mode for each specimen.

Test	$\tau^{max}_{pullout}(\sigma)$ (kPa)	$\tau^{max}_{direct\ shear}(\sigma)$ (kPa)	f_b	Failure mode
T1	17.15	32.82	0.52	Pullout (2) + Tensile (1)
T2	20.55	55.89	0.37	Tensile (3)
T3	13.93	23.01	0.61	Pullout (3)
T4	19.18	41.68	0.46	Tensile (3)
T5	13.29	32.82	0.41	Pullout (3)
T6	16.26	55.89	0.29	Pullout (2) + Tensile (1)
T7	12.16	23.01	0.53	Pullout (3)
T8	16.08	41.68	0.39	Tensile (3)
T9	11.58	32.82	0.35	Pullout (3)
T10	13.77	55.89	0.25	Pullout (3)
T11	10.50	23.01	0.46	Pullout (3)
T12	>17.83	41.68	>0.43	–

It is interesting to point out that the highest pullout resistance was attained for the GGR interface, followed by the GCR and then the GTX (**Table 4**), whereas the corresponding tensile strength values (**Table 2**) followed the reverse trend. This is partly attributed to the interaction mechanisms developed under pullout loading conditions. As stated earlier, in the case of the geogrid, the pullout resistance is composed of frictional resistance (skin friction on the surface of the geogrid longitudinal and transverse ribs) and bearing resistance mobilized against the transverse members. For geotextiles, only the frictional resistance contributes to the overall pullout capacity. Hence, due to the relevance of the passive resistance mobilized under pullout conditions, the geogrid (GGR) presented higher pullout resistance than the remaining geosynthetics (GCR and GTX), despite the comparatively lower tensile strength. Regarding the comparison of results for the GCR and the GTX, this occurrence may be related to the higher extensibility of the geotextile (GTX). Although the ultimate tensile strength of the GTX exceeded that of the GCR, it was achieved at a substantially higher elongation. In fact, the GCR exhibited higher stiffness than the GTX both in the tensile and pullout tests carried out in this study.

From the above observations, it becomes apparent that a geosynthetic with higher tensile strength under unconfined conditions is not necessarily a geosynthetic with better performance when embedded in soil. This highlights the importance of conducting pullout tests with the specific materials to be used in the project if accurate predictions of the geosynthetic pullout capacity are required.

CONCLUSIONS

The pullout behavior of three different geosynthetics (geogrid, geocomposite reinforcement and geotextile) embedded in a locally-available granite residual soil was assessed through a series of large-scale pullout tests involving different soil moisture and density conditions. Based on the analysis of the results, the following conclusions can be drawn.

Soil density is a key factor for the reinforcement pullout resistance, with great influence on the failure mode (pullout or geosynthetic tensile rupture), regardless of geosynthetic type, or soil moisture content.

The soil moisture condition may considerably affect the pullout capacity of geosynthetics, particularly when the soil is in medium dense state. The maximum pullout resistance of the geosynthetics used in this study decreased by up to 19% when the soil was tested at the optimum moisture content, in comparison with the values obtained with dry soil.

The geogrid exhibited higher peak pullout resistance than the remaining geosynthetics, which is associated with the significant contribution of the passive resistance mobilized against the geogrid transverse members to the overall pullout capacity of the reinforcement.

The soil-geosynthetic pullout interaction coefficients ranged from 0.25 to 0.61, with the highest values obtained for the geogrid interface. The occurrence of geosynthetic tensile failure when the specimens were embedded in dense soil is the reason for lower pullout interaction coefficients, comparatively with those generally reported by other researchers.

DATA AVAILABILITY STATEMENT

The raw data supporting the conclusions of this article will be made available by the authors, without undue reservation, to any qualified researcher.

AUTHOR CONTRIBUTIONS

FF performed the pullout tests, analyzed the results and partially prepared the manuscript based on inputs and guidance of CV and ML. CV supervised all the works carried out and modified the initial draft of the manuscript. FF revised the manuscript after peer-review and prepared the final version for publication.

FUNDING

This work was financially supported by the Research Project CDW_LongTerm, POCI-01-0145-FEDER-030452, funded by FEDER funds through COMPETE2020—Programa Operacional Competitividade e Internacionalização (POCI) and by national funds (PIDDAC) through FCT/MCTES.

ACKNOWLEDGMENTS

The authors wish to thank TenCate for providing the geosynthetic samples used in this study. The authors declare that TenCate was not involved in the study design, collection, analysis, interpretation of data, the writing of this article or the decision to submit it for publication.

REFERENCES

Abu-Farsakh, M. Y., Almohd, I., and Farrag, K. (2006). Comparison of field and laboratory pullout tests on geosynthetics in marginal soils. *Transp. Res. Rec.* 1975, 124–136. doi: 10.1177/0361198106197500114

Ashmawy, A. K., and Bourdeau, P. L. (1995). Geosynthetic-reinforced soils under repeated loading: a review and comparative design study. *Geosynth. Int.* 2, 643–678. doi: 10.1680/gein.2.0029

ASTM D 2487-11. (2011). *Standard Practice for Classification of Soils for Engineering Purposes (Unified Soil Classification System)*. West Conshohocken, PA: ASTM International.

ASTM D 4253-93. (1993). *Standard Test Methods for Maximum Index Density and Unit Weight of Soils Using a Vibratory Table*. West Conshohocken, PA: ASTM International.

ASTM D 4254-93. (1993). *Standard Test Methods for Minimum Index Density and Unit Weight of Soils and Calculation of Relative Density*. West Conshohocken, PA: ASTM International.

ASTM D6706-01. (2013). *Standard Test Method for Measuring Geosynthetic Pullout Resistance in Soil*. West Conshohocken, PA: ASTM International.

Bakeer, R. M., Abdel-Rahman, A. H., and Napolitano, P. J. (1998). Geotextile friction mobilization during field pullout test. *Geotext. Geomembranes* 16, 73–85. doi: 10.1016/S0266-1144(97)10024-3

BSI. (1990). *BS 1377-4:1990. Methods of Test for Soils for Civil Engineering Purposes. Compaction-Related Tests*. London: British Standards Institution.

Byun, Y. H., and Tutumluer, E. (2019). Local stiffness characteristic of geogrid-stabilized aggregate in relation to accumulated permanent deformation behavior. *Geotext. Geomembranes* 47, 402–407. doi: 10.1016/j.geotexmem.2019.01.005

CEN. (2004). *EN 13738:2004. Geotextiles and Geotextile-Related Products—Determination of Pullout Resistance in Soil*. Brussels: European Committee for Standardization.

CEN. (2008). *EN ISO 10319:2008. Wide-Width Tensile Tests*. Brussels: European Committee for Standardization.

Esmaili, D., Hatami, K., and Miller, G. A. (2014). Influence of matric suction on geotextile reinforcement-marginal soil interface strength. *Geotext. Geomembranes* 42, 139–153. doi: 10.1016/j.geotexmem.2014.01.005

Ferreira, F. B., Vieira, C. S., and Lopes, M. L. (2015). Direct shear behaviour of residual soil–geosynthetic interfaces—influence of soil moisture content, soil density and geosynthetic type. *Geosynth. Int.* 22, 257–272. doi: 10.1680/gein.15.00011

Ferreira, F. B., Vieira, C. S., and Lopes, M. L. (2016a). "Cyclic and post-cyclic shear behaviour of a granite residual soil-geogrid interface," in *Procedia Engineering, Vol. 143, Advances in Transportation Geotechnics III*, ed A. G. Correia (Amsterdam: Elsevier Ltd), 379–386. doi: 10.1016/j.proeng.2016.06.048

Ferreira, F. B., Vieira, C. S., Lopes, M. L., and Carlos, D. M. (2016b). Experimental investigation on the pullout behaviour of geosynthetics embedded in a granite residual soil. *Eur. J. Environ. Civ. Eng.* 20, 1147–1180. doi: 10.1080/19648189.2015.1090927

Ferreira, F. B., Vieira, C. S., Lopes, M. L., and Ferreira, P. G. (2020). HDPE geogrid-residual soil interaction under monotonic and cyclic pullout loading. *Geosynth. Int.* doi: 10.1680/jgein.19.00057. [Epub ahead of print].

Hatami, K., and Esmaili, D. (2015). Unsaturated soil-woven geotextile interface strength properties from small-scale pullout and interface tests. *Geosynth. Int.* 22, 161–172. doi: 10.1680/gein.15.00002

Hsieh, C., Chen, G. H., and Wu, J.-H. (2011). The shear behavior obtained from the direct shear and pullout tests for different poor grades soil-geosynthetic systems Journal of *GeoEngineering* 6, 15–26.

Indraratna, B., Ferreira, F. B., Qi, Y., and Ngo, T. N. (2018). Application of geoinclusions for sustainable rail infrastructure under increased axle loads and higher speeds. *Innov. Infrastruct. Solut.* 3:69. doi: 10.1007/s41062-018-0174-z

Indraratna, B., Qi, Y., Ngo, T. N., Rujikiatkamjorn, C., Neville, T., Ferreira, F. B., et al. (2019). Use of geogrids and recycled rubber in railroad infrastructure for enhanced performance. *Geosciences*. 9:30. doi: 10.3390/geosciences9010030

Isik, A., and Gurbuz, A. (2020). Pullout behavior of geocell reinforcement in cohesionless soils. *Geotext. Geomembranes* 48, 71–81. doi: 10.1016/j.geotexmem.2019.103506

Lee, K. Z. Z., and Wu, J. T. H. (2004). A synthesis of case histories on GRS bridge-supporting structures with flexible facing. *Geotext. Geomembranes* 22, 181–204. doi: 10.1016/j.geotexmem.2004.03.002

Ling, H. I., Wu, J. T. H., and Tatsuoka, F. (1992). Short-term strength and deformation characteristics of geotextiles under typical operational conditions. *Geotext. Geomembranes* 11, 185–219. doi: 10.1016/0266-1144(92)90043-A

Lopes, M. L., and Ladeira, M. (1996a). Influence of the confinement, soil density, and displacement rate on soil-geogrid interaction. *Geotext. Geomembranes* 14, 543–554. doi: 10.1016/S0266-1144(97)83184-6

Lopes, M. L., and Ladeira, M. (1996b). Role of specimen geometry, soil height and sleeve length on the pull-out behaviour of geogrids. *Geosynth. Int.* 3, 701–719. doi: 10.1680/gein.3.0081

Mirzaalimohammadi, A., Ghazavi, M., Roustaei, M., and Lajevardi, S. H. (2019). Pullout response of strengthened geosynthetic interacting with fine sand. *Geotext. Geomembranes* 47, 530–541. doi: 10.1016/j.geotexmem.2019.02.006

Mitchell, J. K. (1976). *Fundamentals of Soil Behavior*. New York, NY: John Wiley & Sons.

Mohiuddin, A. (2003). *Analysis of Laboratory and Field Pull-Out Tests of Geosynthetics in Clayey Soils* (master's thesis). Faculty of the Louisiana State University and Agricultural and Mechanical College, United States.

Moraci, N., and Recalcati, P. (2006). Factors affecting the pullout behaviour of extruded geogrids embedded in a compacted granular soil. *Geotext. Geomembranes* 24, 220–242. doi: 10.1016/j.geotexmem.2006.03.001

Morsy, A. M., Zornberg, J. G., Han, J., and Leshchinsky, D. (2019). A new generation of soil-geosynthetic interaction experimentation. *Geotext. Geomembranes* 47, 459–476. doi: 10.1016/j.geotexmem.2019.04.001

Ngo, N. T., Indraratna, B., Ferreira, F. B., and Rujikiatkamjorn, C. (2018). Improved performance of geosynthetics enhanced ballast: laboratory and numerical studies. *Proc. Inst. Civ. Eng.* 171, 202–222. doi: 10.1680/jgrim.17.00051

Nimbalkar, S., and Indraratna, B. (2016). Improved performance of ballasted rail track using geosynthetics and rubber shockmat. *J. Geotech. Geoenviron. Eng.* 142:04016031. doi: 10.1061/(ASCE)GT.1943-5606.0001491

Palmeira, E. M. (2004). Bearing force mobilisation in pull-out tests on geogrids. *Geotext. Geomembranes* 22, 481–509. doi: 10.1016/j.geotexmem.2004.03.007

Portelinha, F. H. M., Bueno, B. S., and Zornberg, J. G. (2013). Performance of non-woven geotextile-reinforced walls under wetting conditions: laboratory and field investigations. *Geosynth. Int.* 20, 90–104. doi: 10.1680/gein.13.00004

Raju, M. (1995). *Monotonic and cyclic pullout resistance of geosynthetics* (PhD thesis), University of British Columbia, Vancouver, Canada.

Ravi, K., Dash, S. K., Vogt, S., and Braeu, G. (2014). Behaviour of geosynthetic reinforced unpaved roads under cyclic loading. *Indian Geotech. J.* 44, 77–85. doi: 10.1007/s40098-013-0051-9

Samtani, N. C., and Nowatzki, E. A. (2006). *Soils and Foundations Reference Manual: Volume I. Report No. FHWA-NHI-06-088*. Washington, DC: Federal Highway Administration.

Subaida, E. A., Chandrakaran, S., and Sankar, N. (2008). Experimental investigations on tensile and pullout behaviour of woven coir geotextiles. *Geotext. Geomembranes* 26, 384–392. doi: 10.1016/j.geotexmem.2008.02.005

Tan, S. A., Chew, S. H., Ng, C. C., Loh, S. L., Karunaratne, G. P., Delmas, P., et al. (2001). Large-scale drainage behaviour of composite geotextile and geogrid in residual soil. *Geotext. Geomembranes* 19, 163–176. doi: 10.1016/S0266-1144(01)00005-X

Tang, X., Chehab, G. R., and Palomino, A. (2008). Evaluation of geogrids for stabilising weak pavement subgrade. *Int. J. Pavement Eng.* 9, 413–429. doi: 10.1080/10298430802279827

Tatsuoka, F. (2019). Geosynthetic-reinforced soil structures for railways and roads: development from walls to bridges. *Innov. Infrastruct. Solut.* 4:49. doi: 10.1007/s41062-019-0236-x

Vieira, C. S., Lopes, M. L., and Caldeira, L. M. (2013). Sand–geotextile interface characterisation through monotonic and cyclic direct shear tests. *Geosynth. Int.* 20, 26–38. doi: 10.1680/gein.12.00037

Vieira, C. S., Pereira, P. M., and Lopes, M. L. (2016). Recycled construction and demolition wastes as filling material for geosynthetic reinforced structures. Interface properties. *J. Clean. Prod.* 124, 299–311. doi: 10.1016/j.jclepro.2016.02.115

Wu, J. T. H., Siel, B. D., Chou, N. N. S., and Helwany, H. B. (1992). The effectiveness of geosynthetic reinforced embankments constructed over weak foundations. *Geotext. Geomembranes* 11, 133–150. doi: 10.1016/0266-1144(92)90041-8

Conflict of Interest: The authors declare that the research was conducted in the absence of any commercial or financial relationships that could be construed as a potential conflict of interest.